Possible impacts of the Poyang Lake (China) hydraulic project on lake hydrology and hydrodynamics

Geying Lai, Peng Wang and Lin Li

ABSTRACT

Flow regime change is the leading driving force in the evolution of lacustrine ecological systems. According to the planned water level regulation scheme of the Poyang Lake hydraulic project (PLHP), this research discusses the possible impacts of PLHP on the hydrology and hydrodynamics of Poyang Lake (China) using the method of scenario simulation. The results show that a controlled water level of 11 m would effectively raise the average water level during the low-flow period of the lake in a typical dry year, normal year, and wet year, leading to the decrease of flow velocity in the lake. Those changes were more obvious in regions to the north of Tangyin, especially in the waterway of Poyang Lake into the Yangtze River. The flow field to the north of Tangyin under the scenario with the PLHP was apparently different from that under the scenario without PLHP. Furthermore, the PLHP had a significant impact on the water exchange period of the lake due to the increase in the water storage capacity and the reduction of flow velocity. These results can provide support for further quantitative analysis of water quality and the evolution of ecological systems in the lake affected by the PLHP.

Key words | Environmental Fluid Dynamics Code (EFDC) model, hydraulic project, hydrology and hydrodynamics, numerical simulation, Poyang Lake

Geying Lai (corresponding author)
Peng Wang
Lin Li
Key Laboratory of Poyang Lake Wetland and Watershed Research,
Ministry of Education,
Jiangxi Normal University,
Nanchang 330022,
China
E-mail: *laigeying@126.com*

Geying Lai
School of Geography and Environment,
Jiangxi Normal University,
Nanchang 330022,
China

INTRODUCTION

Lakes are not only an important part of water systems, but also ecosystems with high productivity and biodiversity. Hydraulic projects serve the important social function of promoting regional economic development as well as the ecological service functions of regulating high/low flow and protecting against floods. However, hydraulic projects built in the natural water system of rivers and lakes will inevitably destroy the continuity and the sediment load of the river–lake ecosystem, which can lead to changes in the hydrological regime and has negative impacts on the ecotope (Fu *et al.* 2011).

Poyang Lake, the largest freshwater lake in China and one of two Yangtze River-connected lakes in the Yangtze River system, plays an important role in maintaining regional and national ecological safety, including biodiversity protection as well as flood diversion and storage. The highly dynamic characteristics of the water level in Poyang Lake lead to the formation of a unique landscape composed of lake–wetland and ecological patterns (Hui *et al.* 2008; Feng *et al.* 2012). The impoundment of the Three Gorges Dam has caused major changes to the Yangtze River system, including Poyang Lake. A major consequence of such changes is a weakening in the river forcing on the lake, allowing more lake water to flow into the river from July to March (i.e., an emptying effect) (Zhang *et al.* 2014). This has led to a reduction of water storage in Poyang Lake (Guo *et al.* 2012) that has garnered the attention of Chinese scholars and related governmental departments

doi: 10.2166/nh.2016.174

(Liu *et al.* 2011). Compared to climate variability impacts on the lake catchment, modifications to Yangtze River flows from the Three Gorges Dam have had a much greater impact on the seasonal dryness of Poyang Lake (Hu *et al.* 2007; Zhang *et al.* 2014). The construction of the Poyang Lake hydraulic project (PLHP) has also been proposed (Zhang *et al.* 2014). Although the construction of the PLHP will be helpful in addressing the dryness of Poyang Lake during the dry season, it has raised many concerns among scientists (Li 2009), who believe that the PLHP will have a negative impact on cranes and other wintering waterbirds. The elevated water level would also change the flow field and increase water residence time, leading to deterioration of water quality (Hu *et al.* 2012; Wang *et al.* 2014). The regulation scheme of the PLHP has been modified several times to solve these issues, but the controversy is still ongoing.

Hydrodynamic parameters are the leading driving force in the evolution of river–lake ecosystems (Nikora 2010). The hydrodynamic model is an important and effective tool to conduct quantitative analysis on variations of hydrological regime (Obeysekera *et al.* 2011; Renhua *et al.* 2015), which can effectively assess the impacts of multiple variables on variation of hydrological regime of the river–lake system in a short time. An increasing number of researchers have used hydrodynamic models to study hydrodynamics, eutrophication, and ecological restoration in rivers, reservoirs, lakes, estuaries, and coastal areas (Ferrari *et al.* 2010; Xin *et al.* 2011; Li *et al.* 2013, 2014).

The Environmental Fluid Dynamics Code (EFDC) hydrodynamic model can be used to simulate one-, two-, or three-dimensional flow, transport, and biogeochemical processes in surface water systems including rivers, lakes, estuaries, and reservoirs. The EFDC model was originally developed by the Virginia Institute of Marine Science for estuarine and coastal applications (Hamrick 1992). It is a public domain software that has become one of the most widely used and technically defensible hydrodynamic models (Scott *et al.* 2013; Zhou *et al.* 2014). The model solves three-dimensional, vertically hydrostatic, free surface, and turbulent averaged equations of motion for a variable-density fluid. The EFDC model allows for drying and wetting in shallow areas via a mass conservation scheme. Furthermore, the model is highly flexible. As the software is open source, the underlying code can be easily modified according to a specific application goal. The model was developed using the FORTRAN programming language, which is widely used for computationally intensive tasks.

Using the two-dimensional hydrodynamic model established on the basis of the EFDC model, our study aims to determine: (1) the degree of water level increase in different areas of Poyang Lake caused by the minimum controlled water level (11 m) of the PLHP during the dry season in different typical years; and (2) the possible impacts of the PLHP on the flow field and the water exchange period (WEP) (water residence period) of the lake. The results in this article can provide an essential foundation for the quantitative analysis of the impacts of the PLHP on water quality and ecosystem change.

MATERIALS AND METHODS

Study area

Poyang Lake (28° 40′–29° 46′ N, 115° 49′–116° 46′ E) and its catchment are located in the mid to lower reaches of the Yangtze River (Figure 1). The main inflows of the lake include the Xiuhe River, Ganjiang River, Fuhe River, Xinjiang River, and Raohe River (called the Five Rivers), and the only outlet of the lake is located at Hukou, which is connected with the Yangtze River.

The lake water level ranges from 6 m to 20 m due to the dual effects of seasonal variations in catchment inflows and water level of the Yangtze River. This results in seasonal changes to the lake area, which range from less than 1,000 km^2 in the dry season to over 3,500 km^2 in the rainy season (Min 2000; Tan *et al.* 2013). The wetland of the lake is an important international wetland for its abundant biodiversity. It is one of the ten ecological conservation areas in China, and also one of the globally important ecological areas regulated by the World Wildlife Fund in 1992. The wetland plays an important role in maintaining the ecological safety of the region and the nation.

Poyang Lake is divided into two parts by Songmen Mountain. The northern part is the waterway joining the Yangtze River, and the southern part is the main body of

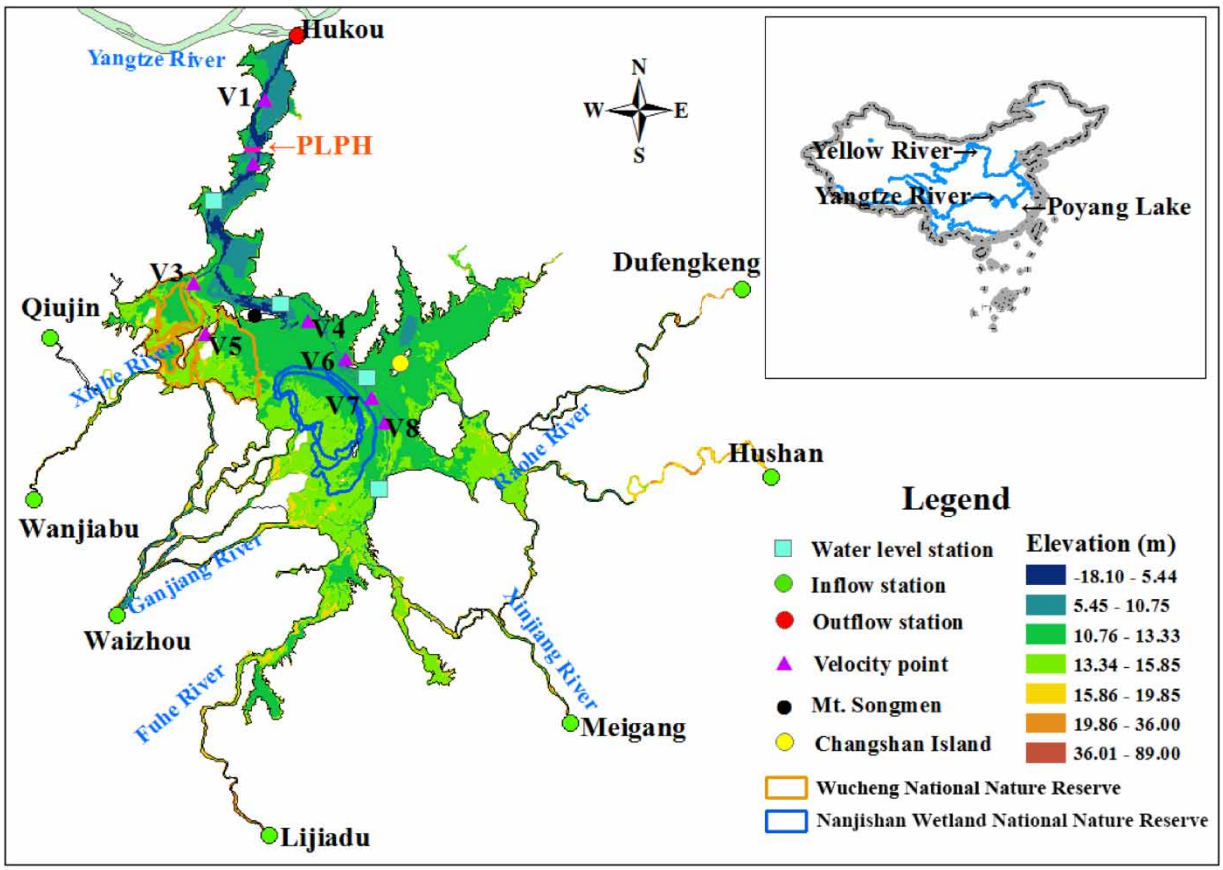

Figure 1 | Map of Poyang Lake. The full color version of this figure is available online and is free to view: http://dx.doi.org/10.2166/nh.2016.174.

the lake. The elevation of the most northernly part is below 12 m, while the bed of the southern part is relatively flat with elevations that are primarily in the range of 12–15 m. Two national nature reserves, the Wucheng National Nature Reserve (WNNR) and the Nanjishan Wetland National Nature Reserve (NWNNR), are located in the Poyang Lake wetland (Figure 1).

Overview of PLHP and its regulation scheme of water level

The proposed PLHP (116 ° 07′ E, 29 ° 32′ N) is located in the waterway that connects Poyang Lake to the Yangtze River (Figure 1). The lake surface of the PLHP site has a width of approximately 2.8 km, which is the narrowest waterway into the Yangtze River. In order to maintain a healthy lake ecosystem and to improve the lake wetland environment, as well as to help relieve some drought issues, a regulation scheme has been proposed (Tan *et al.* 2013) to control the low water level instead of the high water level, and to dynamically adjust the water level (Table 1). In the flood season (from the middle of March to the end of August), the PLHP does not operate, thus allowing free exchanges of water, energy, and biology between the lake and river. From September to October, the water level of the lake will be controlled by the PLHP and will gradually decrease to 11 m. The water level will then be controlled at around 10–11 m from November to the middle of March.

Hydrodynamic governing equations of the model

The EFDC model's hydrodynamic component is based on three-dimensional hydrostatic equations formulated in curvilinear-orthogonal horizontal coordinates and a sigma or stretched vertical coordinate. Its governing equations include momentum, continuity, and transport equations

Table 1 | The scheduling scheme for water level regulation of the PLHP

Date	Regulation scheme
11 Mar.–31 Aug.	All sluices are open, allowing free change of water, energy and organisms, just as in the natural state
1 Sep.–15 Sep.	Water level is controlled at 14 m–15 m after the flood season
16 Sep.–31 Oct.	Water level is decreasing gradually to 12 m from 16 Sep. to 10 Oct.; water level is then decreasing to 11 m from 11 Oct. to 31 Oct.
1 Nov.–10 Jan.	Water level is fluctuating around 11 m
1 Jan.–1 Mar.	Water level is decreasing gradually to 10 m from 11 Jan. to 10 Feb.; then fluctuating between 10 to 11 m from 11 Feb. to 10 Mar.

Note: The water level in the table refers to the elevation of the Yellow Sea, similarly hereinafter.
Source: The data were released by the Water Resources Department of Jiangxi Province on 17 September 2013.

related to salinity and temperature (Hamrick 1992). The momentum equations are as follows:

$$\frac{\partial(mHu)}{\partial t}+\frac{\partial(m_yHuu)}{\partial x}+\frac{\partial(m_xHvu)}{\partial y}+\frac{\partial(mwu)}{\partial z}-\left(mf+v\frac{\partial m_y}{\partial x}-u\frac{\partial m_x}{\partial y}\right)Hv=-m_yH\frac{\partial(g\zeta+p)}{\partial x}-m_y\left(\frac{\partial h}{\partial x}-z\frac{\partial H}{\partial x}\right)\frac{\partial p}{\partial z}+\frac{\partial}{\partial z}\left(m\frac{1}{H}A_V\frac{\partial v}{\partial z}\right)+Q_u \quad (1)$$

$$\frac{\partial(mHv)}{\partial t}+\frac{\partial(m_yHuv)}{\partial x}+\frac{\partial(m_xHvv)}{\partial y}+\frac{\partial(mwv)}{\partial z}+\left(mf+v\frac{\partial m_y}{\partial x}-u\frac{\partial m_x}{\partial y}\right)Hu=-m_xH\frac{\partial(g\zeta+p)}{\partial y}-m_x\left(\frac{\partial h}{\partial y}-z\frac{\partial H}{\partial y}\right)\frac{\partial p}{\partial z}+\frac{\partial}{\partial z}\left(m\frac{1}{H}A_V\frac{\partial v}{\partial z}\right)+Q_v \quad (2)$$

$$\frac{\partial p}{\partial z}=-gH\frac{\rho-\rho_0}{\rho_0}=-gHb \quad (3)$$

where u and v are the horizontal velocity components in the dimensionless curvilinear orthogonal horizontal coordinates x and y, respectively, while w is the vertical velocity in the stretched vertical coordinate z; m_x and m_y are the scale factors of the horizontal coordinates; $m=m_xm_y$ is the Jacobian or square root of the metric tensor determinant; f is the Coriolis parameter; A_v is the vertical turbulent or eddy viscosity; and Q_u and Q_v are momentum source-sink terms. The total water column depth, $H=h+\zeta$, is the sum of the depth below and the free surface displacement relative to the undisturbed physical vertical coordinate origin, $z^*=0$. The pressure p is the physical pressure in excess of the reference hydrostatic pressure, $\rho_0gH(1-z)$, divided by the reference density, ρ_0. The density ρ is generally a function of temperature T and salinity S. b represents the buoyancy, which is defined as the normalized deviation of density from the reference value (Hamrick 1992).

The continuity equations are as follows:

$$\frac{\partial(m\zeta)}{\partial t}+\frac{\partial(m_yHu)}{\partial x}+\frac{\partial(m_xHv)}{\partial y}+\frac{\partial(mw)}{\partial z}=0 \quad (4)$$

$$\frac{\partial(m\zeta)}{\partial t}+\frac{\partial(m_yH\int_0^1 udz)}{\partial x}+\frac{\partial(m_xH\int_0^1 vdz)}{\partial y}=0 \quad (5)$$

$$\rho=\rho(p,S,T) \quad (6)$$

Evaporation from the lake surface is calculated by evaporation heat transfer using the surface heat exchange model:

$$\varphi_n=\varphi_{sn}+\varphi_{anr}-\varphi_e-\varphi_c \quad (7)$$

where φ_n is the heat flux; φ_{sn} is the short-wave solar radiation; φ_{anr} is the net long-wave back radiation; φ_e is the evaporation heat transfer; φ_c is the convective heat transfer.

Establishing a two-dimensional hydrodynamic model for Poyang Lake

Based on the remote sensing image of Poyang Lake taken during the flood period in 1998 and the GIS levee data of the lake, the maximum boundary of the Poyang Lake water surface was determined, which was used as the border of the model domain. A curvilinear orthogonal mesh was used in the model. The total number of grids was 96,004, the mesh resolution ranged from 178 m to 205 m, and the orthogonality parameter of the grid was

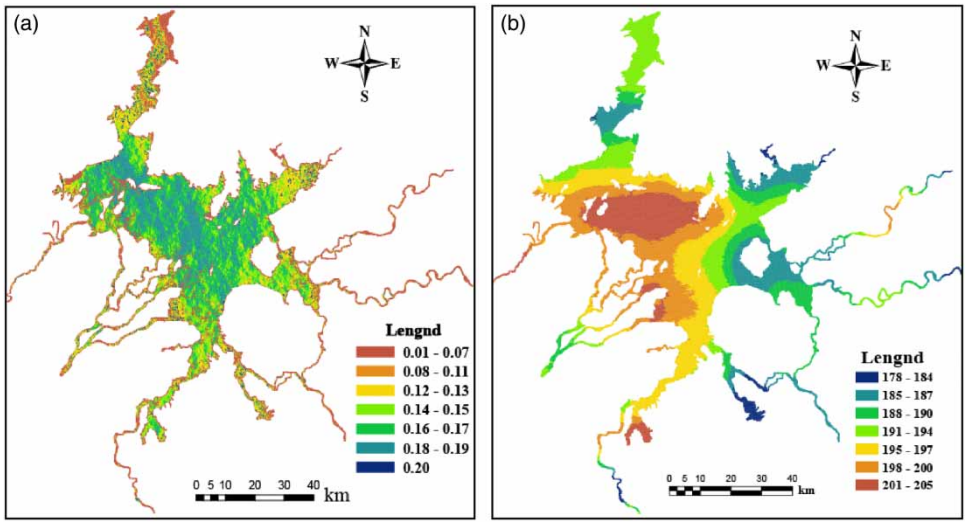

Figure 2 | Parameters of the Poyang Lake hydrodynamic model: (a) orthogonality; (b) resolution (m). The full color version of this figure is available online and is free to view: http://dx.doi.org/10.2166/nh.2016.174.

less than 0.2 (Figure 2(a) and 2(b)). Since most of the grids were non-square, the mesh resolution is represented by the square root of the area of a grid.

The variation of the Poyang Lake bed topography was considered when establishing the model mesh. According to Figure 2(b), since the variation of the bed topography was larger in the northern and the eastern parts of the lake, smaller grids were used to reflect the terrain elevation variation of the lake bed. However, larger grids were used in the floodplain of the lake (at the center of the lake) so that the total number of grids could be controlled and the calculation time could be reduced. The bed topography data for Poyang Lake were collected in 1998 and 2010 at scales of 1:25,000 and 1:10,000, respectively, and were provided by the Changjiang Water Resources Commission and the Water Resources Department of Jiangxi Province, respectively.

Poyang Lake is a shallow lake. Hu *et al.* (2012) considered Poyang Lake as a two-dimensional water body by calculating the morphometric parameters of the lake. A two-dimensional model was also used in this study for simplification and computational efficiency. The Mellor–Yamada level 2.5 turbulence closure schemes (Mellor & Yamada 1982) were employed in the model. The flow boundary in the model was set up using daily inflow data (m^3/s) recorded at hydrological stations on the five tributaries of Poyang Lake (Figure 1). Those hydrological stations included Wanjiabu for Xiuhe River, Waizhou for the Ganjiang River, Lijiadu for the Fuhe River, Meigang for the Xinjiang River, as well as Dufengkeng and Hushan for the Raohe River. However, the drainage area in the downstream of the five gauging stations (about 15.5% of the whole catchment area) has no gauged data. A factor 1.1834, which was calculated by the ratio of total drainage area to gauged drainage area, is introduced to balance the inflow and outflow. As little groundwater data are accessible in the study area, and groundwater only accounts for 1.3% of the total water balance in Poyang Lake (Feng *et al.* 2011), groundwater was neglected in the model. The open boundary was set up using the daily water level records (using meter units and the elevation of the Yellow Sea) at Hukou station. The time-related meteorological conditions, including daily precipitation, wind speed and direction, air temperature, air pressure, relative humidity, and cloud cover, were collected at the hydrologic stations mentioned above. The initial condition of the model was the measured water levels of Hukou, Xingzi, Duchang, Tangyin, Kangshan, and Wucheng (Ganjiang River) hydrological stations at the start time of simulation.

Calibration and verification of the model

Since simulation is time-consuming, the selected parameter calibration duration of the model was set to range from 1 November 1999 to 31 July 2000. Two seasons of high and

Table 2 | Calibrated parameters and optimal values

Parameter	Initial value	Bounds	Calibrated value
Bottom roughness height (m)	0.2	0.01–0.4	0.2 for lake bed; 0.25 for floodplain
Horizontal eddy viscosity (m^2/s)	0.1	0.01–0.4	0.25
Wet depth (m)	0.1	0.01–0.2	0.06

low water level were included in that duration to improve the simulation of high water level and low water level and to improve the efficiency of parameter calibration. The first 2 months of the selected parameter calibration duration were used for the model warm-up period. The calibrated main parameters of the model are shown in Table 2. Four hydrological stations (Xingzi, Duchang, Tangyin, and Kangshan) that continuously measure daily water levels range from the south to the north and cover the entire range of water levels in Poyang Lake (Figure 1). These observed daily water levels were used to calibrate parameters, and the error analysis of calibration for the model is shown in Table 3.

In order to validate the calibrated parameters of the model, the 5 years from 1 January 1999 to 31 December 2003 were selected as the model verification duration. The model was verified by using continuously measured daily water levels at four hydrological stations (Xingzi, Duchang, Tangyin, and Kangshan). Figure 3 provides the comparison of measured water levels and simulated water levels at the four verification sites during the verification period of the model. Ten variables were included in a subsequent error analysis, and the results are shown in Table 4. Mean

Table 3 | Error analysis of model calibration

Sites	Mean water level measured (m)	Mean water level simulated (m)	Minimum water level measured (m)	Minimum water level simulated (m)	Maximum water level measured (m)
Xingzi	10.705	10.465	6.630	6.160	16.150
Duchang	11.580	11.339	8.000	8.085	16.120
Tangyin	12.437	12.150	9.800	9.680	16.200
Kangshan	13.178	12.642	11.000	10.430	16.070

Sites	Maximum water level Simulated (m)	Mean absolute error (m)	Mean relative error (%)	RMS error	Nash–Sutcliffe coefficient (Krausel *et al.* 2005)
Xingzi	16.109	0.281	3.421	0.411	0.981
Duchang	16.133	0.278	2.696	0.378	0.975
Tangyin	16.120	0.290	2.510	0.371	0.962
Kangshan	16.125	0.560	4.475	0.635	0.808

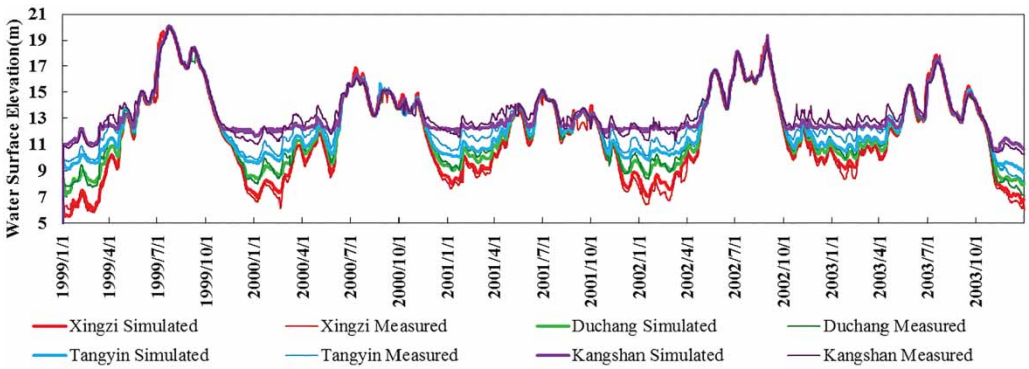

Figure 3 | Daily measured and simulated water levels of model verification. The full color version of this figure is available online and is free to view: http://dx.doi.org/10.2166/nh.2016.174.

Table 4 | Error analysis of model validation

Sites	Mean water level measured (m)	Mean water level simulated (m)	Minimum water level measured (m)	Minimum water level simulated (m)	Maximum water level measured (m)
Xingzi	11.657	11.845	5.860	5.516	20.000
Duchang	12.335	12.273	7.090	7.130	20.000
Tangyin	12.972	12.648	8.170	8.710	20.080
Kangshan	13.522	13.417	10.230	10.500	19.980

Sites	Maximum water level simulated (m)	Mean absolute error (m)	Mean relative error (%)	RMS error	Nash–Sutcliffe coefficient
Xingzi	20.046	0.234	2.478	0.351	0.989
Duchang	20.070	0.221	2.062	0.303	0.988
Tangyin	20.070	0.393	3.353	0.513	0.950
Kangshan	20.070	0.321	2.481	0.412	0.951

absolute error in Table 4 is the average value of the difference between the daily measured water level and the simulated water level.

The daily measured flow velocity and flow direction datasets were not available for the study area. Two datasets of flow velocity and flow direction at eight sites (see V1–V8 in Figure 1) were used to validate the simulated results. These data were collected by the Water Resources Department of Jiangxi Province during a low water level period (28–29 December 2010) and a high water level period (9–11 October 2010). The position, observation date, flow velocity, flow direction, and related validation information at the eight sites are shown in Table 5. The two values in the bracket in column 4 of Table 5 refer to the two simulated velocity components in the x and y directions, respectively.

Figure 3 and Table 4 show that the mean error at the four sites varied from 0.234 m to 0.393 m, the relative error ranged from 2.062% to 3.353%, the root-mean-square (RMS) error ranged from 0.303 to 0.513, and the Nash–Sutcliffe efficiency coefficient ranged from 0.950 to 0.989. The errors of Xingzi site and Duchang site were proximate to each other. The errors of Tangyin and Kangshan exhibited a large difference, which might relate to a mismatch between the grid size and topographic variability in Tangyin and Kangshan. Compared with other sites, the bed topographies of Tangyin and Kangshan were more complex because of greater elevation variability (Figure 1). Furthermore, the grids of the model had coarser resolution in Kangshan compared with those of other sites (Figure 2(b)), thus the resolution of the grids in Tangyin and Kangshan did not properly reflect the elevation variability of the actual topography. In addition, the measured water levels of Kangshan from November 1999 to May 2000, from December 2000 to May 2001, from December 2001 to May 2002, and from December 2002 to April 2003 were highly variable (Figure 3), while the simulated water levels were much more stable. The reason might be that the terrain was flattened after interpolation. A combination of the two causes above resulted in significant error between the measured value and simulated value at the Kangshan site.

According to Table 5, the site with the maximum error was V8 (29 December), and its error and relative error were 0.403 m/s and 30.3%, respectively. The site with the minimum error was V3 (11 October), and its error and relative error was −0.017 m/s and −3.8%, respectively. For flow direction, the site with the maximum error (37.3 °) was V8 (29 December) and the site with the minimum error (0.9 °) was V2 (28 December). The mean error of velocities at the eight sites was 0.106 m/s, the mean relative error was 13.3%, and the mean error of flow direction was 7.8 °. In the high water level period, the mean error of the velocity was 0.054 m/s, the mean relative error was 12.9%, and the mean error of flow direction was 5.8 °. In the low water level period (December), the mean error of the velocity was 0.158 m/s, the relative error was 13.8%, and the mean error of flow direction was 9.9 °. Thus, the velocity and flow direction errors of the simulation results in the high water level period (October) were lower than those in the low water level period.

Table 5 | Verification of current velocity and direction

Time	Location	Measured flow velocity (m/s)	Simulated flow velocity (m/s) (x, y)	Error	Relative error (%)	Measured flow direction (degree)	Simulated flow direction (degree)	Error
10 Oct.	V1	0.104	0.131 (0.064, 0.114)	−0.027	−26.0	37.7	29.3	8.4
9 Oct.	V2	0.537	0.419 (− 0.210,0.363)	0.118	22.0	338.9	330.0	8.9
11 Oct.	V3	0.445	0.462 (− 0.178, 0.426)	−0.017	−3.8	325.9	337.3	−11.4
10 Oct.	V4	0.387	0.332 (− 0.208, 0.259)	0.055	14.2	322.3	321.2	1.1
9 Oct.	V5	0.397	0.373 (0.345, 0.338)	0.024	6.0	39.7	45.6	−5.9
10 Oct.	V6	0.744	0.692 (− 0.662, 0.201)	0.052	7.0	294.6	286.9	7.7
11 Oct.	V7	0.600	0.480 (− 0.308, 0.368)	0.120	20.0	321.5	320.1	1.4
11 Oct.	V8	0.500	0.479 (− 0.063, 0.475)	0.021	4.2	353.7	352.4	1.3
Date	**Location**	**Measured flow velocity(m/s)**	**Simulated flow velocity (m/s) (x, y)**	**Error**	**Relative error (%)**	**Measured flow direction (degree)**	**Simulated flow direction (degree)**	**Error**
28 Dec.	V1	0.515	0.473 (0.244, 0.407)	0.042	8.2	37.3	30.9	6.4
28 Dec.	V2	0.791	0.728 (0.098, 0.701)	0.063	8.0	8.9	8.0	0.9
28 Dec.	V3	1.060	1.10 (− 0.222, 1.079)	−0.040	−3.8	341.4	348.4	−7.0
29 Dec.	V4	1.050	0.941 (− 0.559, 0.757)	0.109	10.4	321.3	323.6	−2.3
29 Dec.	V5	1.190	1.05 (0.722, 0.768)	0.140	11.8	46.33	43.3	3.0
29 Dec.	V6	1.040	0.942 (− 0.559, 0.757)	0.098	9.4	326.5	323.6	2.9
28 Dec.	V7	1.290	0.923 (− 0.564, 0.731)	0.367	28.4	341.4	322.4	19.0
29 Dec.	V8	1.330	0.927 (− 0.572, 0.731)	0.403	30.3	359.4	322.1	37.3

To better verify the reliability of the simulation results, it is necessary to contrast the simulated water surface with the actual water surface. Figure 4 shows the comparison between two groups of simulated lake water depth distributions and lake water surfaces from remote sensing images taken during low/high water level periods. Figure 4(a) and 4(b), respectively, illustrate the simulated water surface and the actual water surface extracted from the remote sensing image on 10 December 1999. Figure 4(c) and 4(d) show the simulated water surface and the actual water surface extracted from the remote sensing image on 23 September 2000, respectively. According to the comparisons of Figure 4(a) with 4(b) and Figure 4(c) with 4(d), the simulated water surfaces and the actual water surfaces exhibit a high level of correspondence.

Scenario simulation scheme

In order to study the benefits and impacts of the PLHP on hydrological conditions and dynamics, two scenarios were generated. The first is the base scenario (termed S1), in which there is no PLHP in the lake. The second scenario (denoted as S2) is an unnatural-state lake with normal inflow and meteorological conditions but with a water level regulated by the PLHP as an outflow condition. In the above two scenarios all boundary conditions, except the outflow condition, are the same. Therefore, we assume that if there is any difference in the results of the two scenarios, the difference is caused by the water level regulation of the PLHP.

The flow boundary condition, the open boundary condition, and the meteorological conditions for the S1 scenario were equal to those used in the calibration and verification simulation, while the simulation duration, corresponding data of flow and water level, and the initial conditions differed. The boundary conditions of the S2 scenario were equal to those of S1, except for the open boundary condition. The open boundary condition of S2 was the forcing water level at the site of the PLHP. Since no corresponding gauging station was constructed at the site of the PLHP, the water level at the site of the PLHP had to be obtained according to the following rule. The water level at the site of the PLHP consisted of the daily water level simulated by scenario S1 at the site of the PLHP in the period from March 16 to August 31 and the regulation water level specified in the PLHP scheduling scheme in the rest days, which excluded the days when the simulated water level of scenario S1 at the site of the PLHP was greater than the regulation water level specified in the PLHP scheduling scheme.

Typical hydrological years from 2000 to 2013 for scenario design included wet year, normal year, and dry year, and the selection for three typical years was based primarily on the average water level and total flow of the lake outlet from November 1 of one year to March 15 of the next year according to the planning for operation of water levels for the PLHP. Therefore, 2003, 2006, and 2010 were selected as the dry, normal, and wet years, respectively. For these three periods, the average water levels of the lake outlet in the period from November 1 of the current year to March 15 of the following year were 6.08 m, 6.41 m, and 7.42 m, respectively. The total flows in the same period were 1.47×10^{10} m^3, 2.38×10^{10} m^3, and 2.59×10^{10} m^3, respectively. The time of scenario simulation for each typical year was from January 1 of the current year to July 31 of the following year, and the warm-up

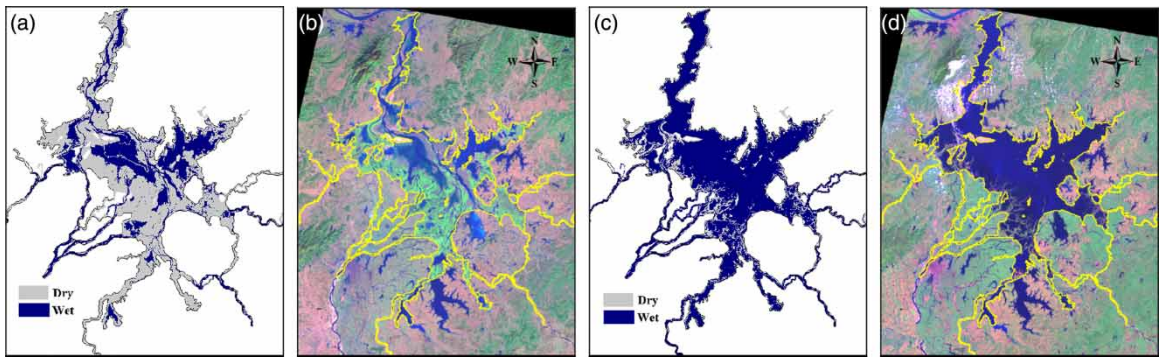

Figure 4 | Comparison between simulated lake surface and water surface in satellite image: (a) simulated water surface of 10 December 1999; (b) satellite image of water surface on 10 December 10 1999; (c) simulated water surface of 23 September 2000; (d) satellite image of water surface on 23 September 2000. The full color version of this figure is available online and is free to view: http://dx.doi.org/10.2166/nh.2016.174.

period for the modeling was 2 months from 1 November to 31 December of the previous year.

RESULTS AND ANALYSIS

Water level increase caused by the minimum control water level (11 m) of the PLHP in low-flow periods

Since 2000, problems such as the temporal advance of low-flow periods, relatively low water levels, and longer low-flow period duration have occurred in Poyang Lake. These problems are due to many causes, such as reduction of runoff into the Poyang Lake and variation in the water resource situation of the Yangtze River. To mitigate these impacts, a minimum control water level of 11 m is planned in the regulation scheme of the PLHP for the low-flow period from November 1 of a certain year to mid-March of the following year.

Figure 5 shows the degree of uplift and the spatial distribution of mean lake water level caused by the control water level of 11 m during the low level ecological regulation period (from November 1 of each year to March 15 of the following year) of the PLHP in typical years. In 2010 (the wet year), the maximum uplift in mean lake water level during the low-flow period was 3.07 m. In 2006 (the normal year), the maximum increase was 3.94 m. In 2003 (the dry year), the maximum increase was 4.50 m. In addition, the northern part of the lake near Songmen Mountain exhibited the largest average uplift of water level. The uplift of average water level in other areas was very small, and in the two national nature reserves, WNNR and NWNNR, there was little increase in the average water level. Therefore, the control water level of 11 m made certain contributions to regulating the lake water level during the low-flow period of different hydro-scenario years, especially the dry year. An uplift in water level during the low-flow period could solve related problems such as the temporal advance of the low-flow period, low water levels, and the increasing duration of the low water level period.

Analysis of impacts of the PLHP on lake flow field

In order to conduct a contrastive analysis of the PLHP impacts on the flow velocity of Poyang Lake, 204 model grids were selected as observation points. These points were distributed in six regions of the model's computing domain, namely, the waterway into the Yangtze River (7 points), north of Tangyin (28 points), south of Tangyin (21 points), WNNR (72 points), NWNNR (64 points), and the vicinity of Changshan Island (12 points). The simulated flow velocities for the S1 and S2 scenarios at these points were used to analyze and compare differences between the

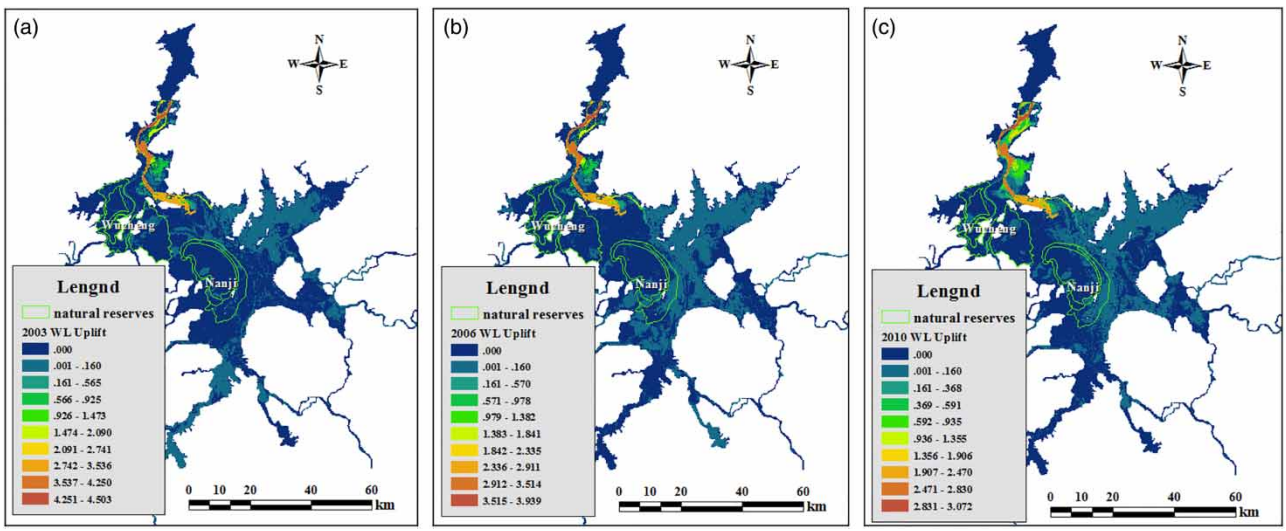

Figure 5 | Uplift distribution of average water level of Poyang Lake during low-flow period in different scenario years as caused by the minimum control water level of 11 m: (a) 2003 (dry year); (b) 2006 (normal year); (c) 2010 (wet year). The full color version of this figure is available online and is free to view: http://dx.doi.org/10.2166/nh.2016.174.

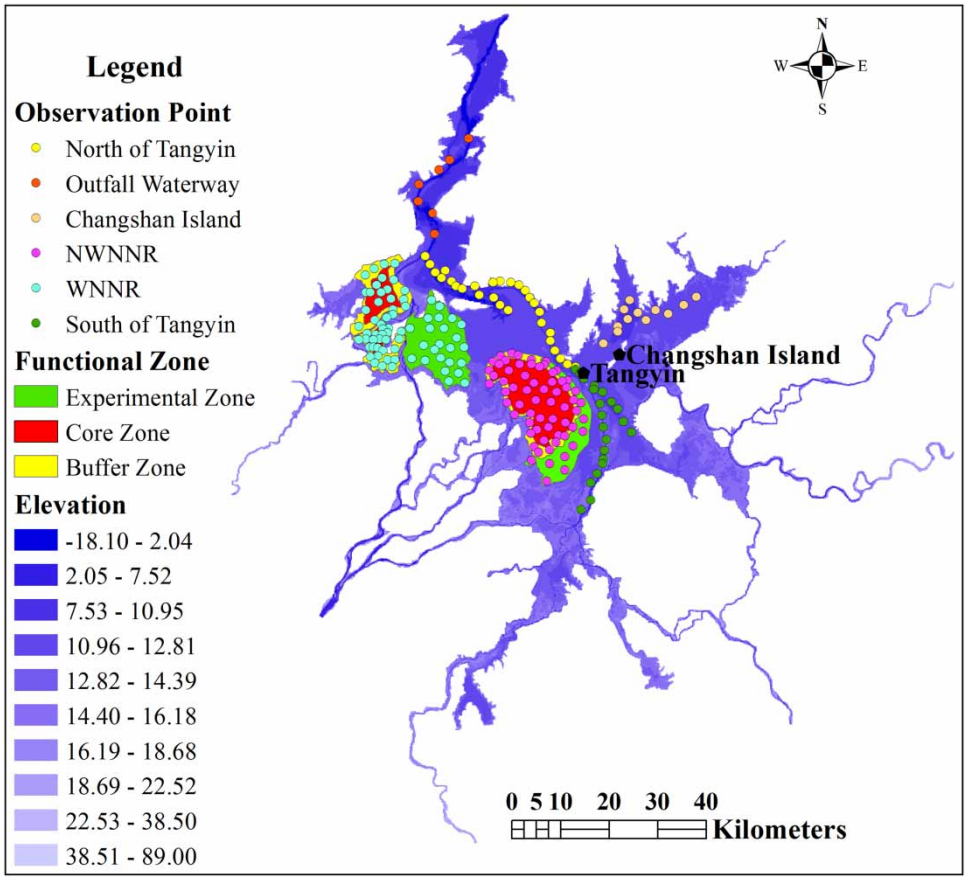

Figure 6 | Distribution of observation points. The full color version of this figure is available online and is free to view: http://dx.doi.org/10.2166/nh.2016.174.

scenarios. Figure 6 shows an illustration of the distribution of the selected observation points.

Figure 7 shows a comparison diagram for the maximum velocities, the minimum velocities, and mean velocities of different lake regions in every month. The figure also shows these parameters for the water-level regulation periods (WLRP) (from September 1 to March 15 of the following year) in a typical wet year, normal year, and dry year, which were based on the simulation results under the S1 and S2 scenarios. Figure 7 indicates that the water-level regulation process of the PLHP created different impacts on velocities in the different lake regions. The impacts on the waterway into the Yangtze River were the greatest; impacts on regions between the waterway and Tangyin were intermediate; and impacts on regions in southern Tangyin, the vicinity of Changshan Island, and in the two natural reserve areas were small.

The maximum velocities and monthly mean velocities of the waterway that flowed into the Yangtze River in years of different types decreased significantly, but the minimum velocities changed slightly. During the WLRP in 2003, the maximum velocity and the mean velocity in the Yangtze River waterway under the S1 scenario were 0.93 m/s and 0.26 m/s, respectively, while those under the S2 scenario were 0.65 m/s and 0.15 m/s, respectively. Therefore, compared with the velocities under the scenario of S1, the maximum velocity and the mean velocity under the S2 scenario decreased by 30.1% and 41.1%, respectively. In 2006, the maximum velocity and the mean velocity under the S1 scenario for WLRP in the Yangtze River waterway were 0.90 m/s and 0.40 m/s, respectively, and those values under the S2 scenario were 0.72 m/s and 0.22 m/s, respectively. Therefore, compared with the velocities under the S1 scenario, the maximum velocity and the mean velocity

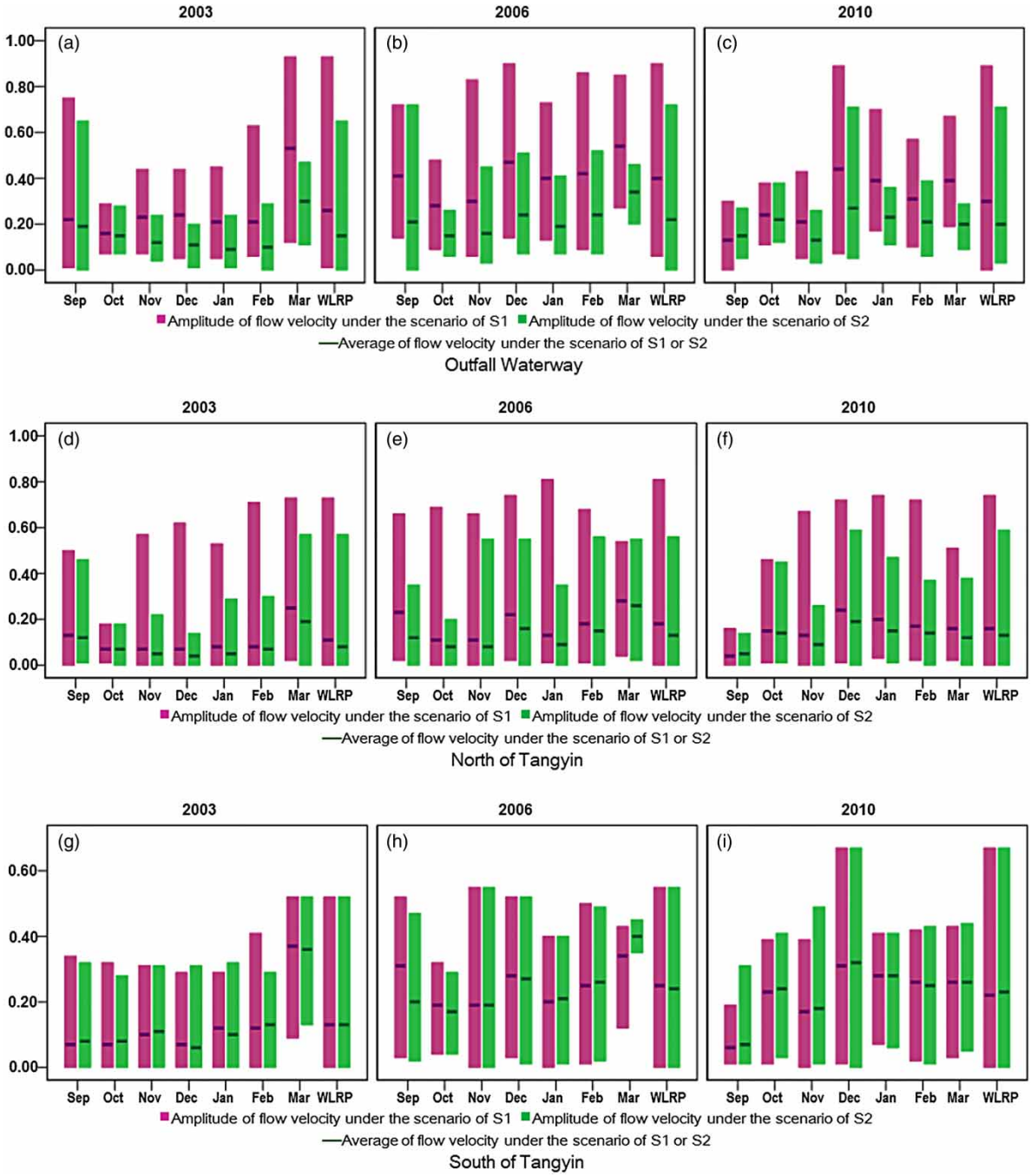

Figure 7 | Maximum, minimum, and mean of velocities in several important lake regions under the scenario with/without hydraulic project in a full year, low-water level and high-water level period. The full color version of this figure is available online and is free to view http://dx.doi.org/10.2166/nh.2016.174. *(Continued.)*

under the S2 scenario decreased by 20.0% and 45.7%, respectively. In 2010, the maximum velocity and the mean velocity during the WLRP under the S1 scenario in the Yangtze River waterway were 0.89 m/s and 0.30 m/s, respectively, and those values under the S2 scenario were 0.71 m/s and 0.20 m/s, respectively. Therefore, compared with the velocities under the S1 scenario, the maximum velocity and the mean velocity under the S2 scenario decreased by 20.2% and 33.2%, respectively. The rate of decrease in mean velocities under the S2 scenario was 45.7% in 2006

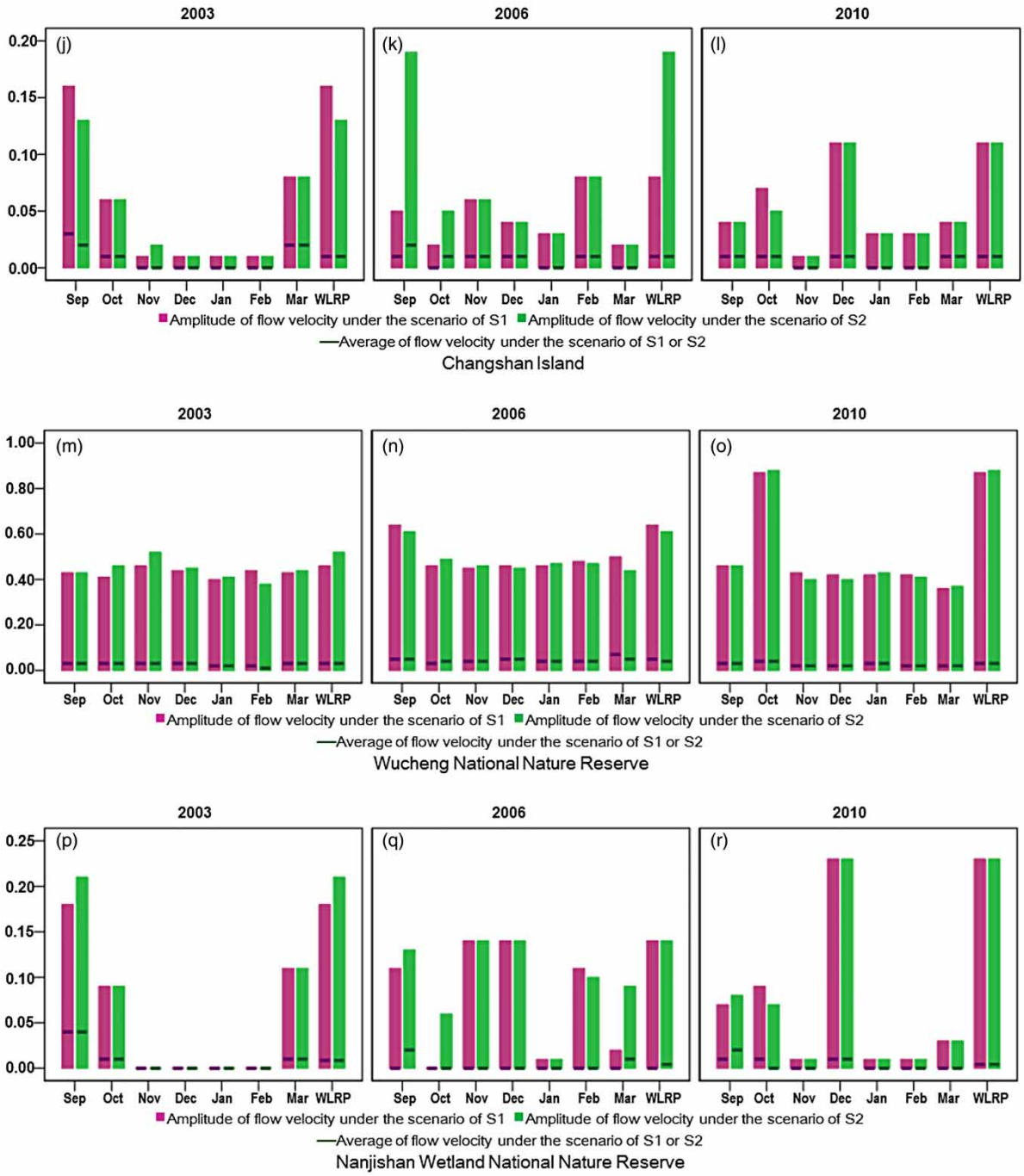

Figure 7 | Continued.

(the normal year), which was higher than that in 2003 (the dry year). In addition, from Figure 7(a)–7(r) it can be seen that the month with the maximum rates of decrease in maximum velocity and in the mean velocity under the S2 scenario varies in different years.

To the north of Tangyin, the rates of decrease in the maximum velocities and monthly mean velocities for the years of different scenarios were relatively small, and the minimum velocities generally remained stable. In 2003, the maximum velocity and the mean velocity at this location

in WLRP under the S1 scenario were 0.73 m/s and 0.11 m/s, respectively, and these values were 0.57 m/s and 0.08 m/s, respectively, under the S2 scenario. Therefore, the maximum velocity and the mean velocity under the S2 scenario decreased by 21.9% and 21.3%, respectively. In 2006, the maximum velocity and the mean velocity at this location in WLRP were 0.81 m/s and 0.18 m/s, respectively, under the S1 scenario, and these values were 0.56 m/s and 0.13 m/s, respectively, under the S2 scenario. Comparing the velocity under the S2 scenario with that under the S1 scenario, the rates of decrease in the maximum velocity and the mean velocity were 30.9% and 25.4%, respectively. In 2010, the maximum velocity and the mean velocity at this location in WLRP were 0.74 m/s and 0.16 m/s, respectively, under the S1 scenario, and these values were 0.59 m/s and 0.13 m/s, respectively, under the S2 scenario. Comparing the velocity under the S2 scenario with that under the S1 scenario, the rates of decrease in the maximum velocity and the mean velocity were 20.3% and 19.3%, respectively.

As shown in Figure 7(g)–7(r), the velocity under the S1 scenario and that under the S2 scenario changed slightly. This indicates that the regulation scheme of the PLHP for water level (especially the water level of 11 m) caused negligible impacts on the velocities in lake regions including south of Tangyin, Changshan Island, WNNR, and NWNNR, due to the high terrain of the lake bed.

However, the results also show that among the 3 year types (dry year, normal year, and wet year) the rate of decrease in velocity, either maximum velocity or mean velocity, did not show obvious regularity in different regions of the lake under the S2 scenario. For example, as a normal year, the decrease in velocity caused by the PLHP in 2006 should be less than that in 2003 (dry year). However, there was a greater decrease of velocity in 2006 than that in 2003, and there was less decrease in 2006 than that in 2010 (wet year). These results seem to indicate that although the PLHP caused a change of flow velocity, this change was unrelated to hydro-year types (dry year, normal year, and wet year). However, this is a false impression. As stated above, 2003, 2006, and 2010 were selected as the dry year, normal year, and wet year mainly based on their average water levels and the total flow at Hukou in the period from November 1 of that year to March 15 of the following year. Figure 8 shows monthly mean flow and monthly water level during the WLRP in years of different types. From the figure it can be seen that the monthly mean flow from November of 2006 to March of the following year was greater than that in the same period of 2003. However, the monthly mean water level in 2006 was close to the monthly mean water level in 2003, and at some points the monthly mean water level in 2006 was less than the monthly mean water level in 2003 (e.g., November) (Figure 8). Generally, the lower the water level and the greater the flow at Hukou, the greater the slope of the water surface and the flow velocity in Poyang Lake. Therefore, it is reasonable that the change in the flow velocity in 2006 was greater than that in 2003 due to the impact of the PLHP.

To summarize, the PLHP might have different impacts on the mean velocity, the maximum velocity, and the minimum velocity in different regions of the lake during the WLRP. The impacts on the waterway into the Yangtze

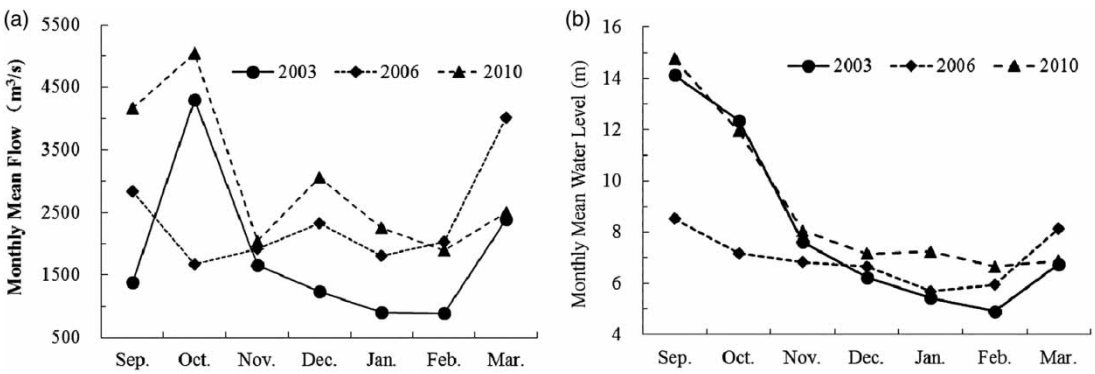

Figure 8 | Monthly mean flow and monthly water level during regulating water-level period in years of different types: (a) monthly mean flow; (b) monthly mean water level.

River were the greatest, and the impacts on the two natural reserve areas were relatively small.

The water level in Poyang Lake is determined by both the basin inflow and the water level in the Yangtze River, and the water in the Yangtze River may flow backwards to Poyang Lake when its water level is high due to flood. The main form of lake current is influent–effluent current. Furthermore, the lake rarely exhibits a density current. The influent–effluent current can be further classified into currents of gravity type, backward flow type, and top-lifted type based on the flow conditions, flow direction, and hydrological relation between Poyang Lake and the Yangtze River. Among the above three types of lake currents, the gravity current occupies the largest proportion. Generally, the backward flow lake current type exists in the period from July to October, when the flood season of the Five Rivers is generally over. During this period, the water level of the Yangtze River increases rapidly and becomes higher than the water level of Poyang Lake, and Poyang Lake has a relatively small water surface slope. The top-lifted type of lake current mainly exists during the flood season, when the Five Rivers and the Yangtze River simultaneously flood. The top-lifted type of lake current also occurs when the flood season of the Five Rivers is over but flooding of the Yangtze River is insufficient for backward flow into Poyang Lake (Tan *et al.* 2013). According to the scheduling scheme of the PLHP in Table 1, the water level regulation process is mainly effective during the period from September 1 of each year to the middle of March in the following year, in which the flood season is not included. Therefore, the hydraulic project will cause no impacts on the top-lifted type of lake current. Although the backward flow type period of lake current and the water-level regulation process period partially overlap (from September to October), the backward flow type of lake current is not affected by the PLHP because the scheduling scheme of the PLHP is mainly based on the principle of control over low flow instead of controlling floods. Therefore, only the impacts of the gravity flow field are considered when discussing the impacts caused by the PLHP on the flow field of the lake.

To further analyze and discuss the impacts caused by the PLHP on the gravity flow field of the lake, the flow fields with the lowest water level under the S1 scenario and the flow fields under the S2 scenario on the same day during the WLRP of the PLHP were selected for comparison. The specific times were 4 February 2004, 15 February 2007, and 13 December 2010, respectively, and the corresponding simulated water levels at Xingzi were 4.61 m, 4.72 m, and 6.11 m, respectively. Figure 9 shows the situations of the flow fields with the lowest water level under the S1 scenario in these typical years and those under the S2 scenario in the same period (vector and scalar). Figure 9(a)–9(c), respectively, show the flow fields of the lake with the lowest water level under the S1 scenario, and Figure 9(d)–9(f) show the flow fields on the same day in the corresponding year under the S2 scenario.

According to Figure 9(a)–9(c), the lowest water levels in years of different types under the S1 scenario varied, but the flow fields were in similar situations. The main lake region appeared to exhibit a 'fluvial facies' type flow field. Due to the confluence of two rivers, the backflow field (see Figure 9(a)) might occur easily in the lake region proximate to Changshan Island when there is a large quantity of water outlets from the two rivers. According to Figure 9(d)–9(f), the flow fields were similar when the water level was regulated to 10–11 m under the S2 scenario. However, the waterway joining the Yangtze River under the S2 scenario exhibited a complex flow field due to the increase in water level, and the flow field was relatively weakened under the S2 scenario (comparing Figure 9(b) with Figure 9(c), 9(e) and 9(f)). When comparing Figure 9(a) and 9(d), the flow fields of the region close to Changshan Island varied greatly, i.e., this region exhibited a backflow field under the S1 scenario and a conventional flow field under the S2 scenario. This result is due to the fact that the water level at the site of the PLHP under the S2 scenario was regulated from 10 to 11 m on February 4, and the drainage process resulted in the disappearance of the backflow fields in the region near Changshan Island.

Analysis of impacts of the PLHP on the WEP of Poyang Lake

The monthly WEPs during the WLRP in different types of years were calculated based on the concept of WEP. The calculation formula used is as follows:

$$p_l = \frac{\sum_{i=1}^{T}\sum_{j=1}^{n}\xi_j H_{ij}}{86400 \times \sum_{i=1}^{T}\sum_{k=1}^{m} Q_{ik}}, \quad if \quad Q_{ik} < 0, \quad Q_{ik} = 0 \tag{8}$$

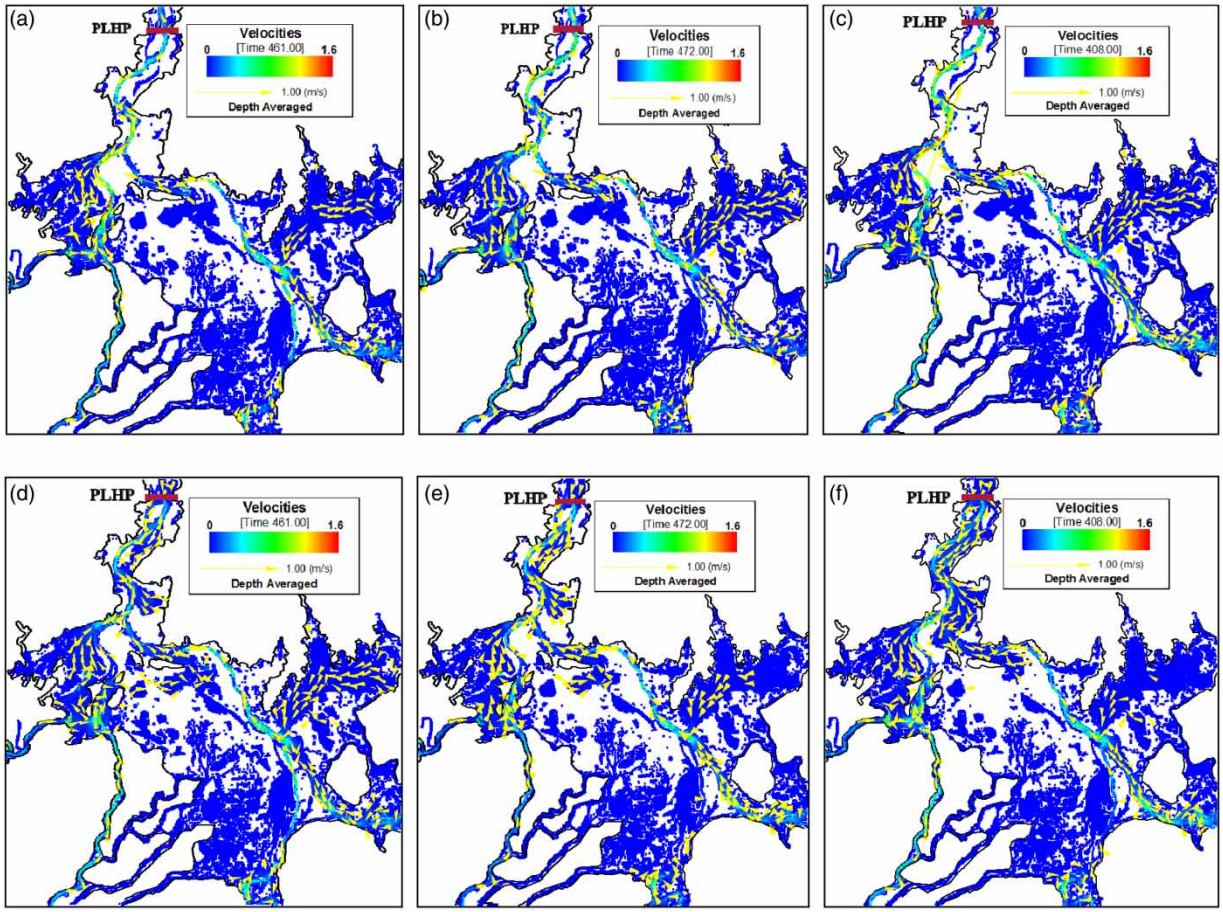

Figure 9 | Comparison of flow fields under the S1 and S2 scenarios during the lowest water level in typical years: (a) flow field under the S1 scenario during a dry year; (b) flow field under the S1 scenario in a normal year; (c) flow field under the S1 scenario during a wet year; (d) flow field under the S2 scenario in a dry year; (e) flow field under the S2 scenario in a normal year; (f) flow field under the S2 scenario in a wet year. The full color version of this figure is available online and is free to view: http://dx.doi.org/10.2166/nh.2016.174.

where P_l is the water exchange period of the lth month, ξ is the area of grid j (m^2), H is the simulated mean water depth of grid j on the ith day (m), n is the number of grids over the whole computational domain of the lake (96,004), Q_{ik} is the simulated flow of grid k at the outlet section (m^3/s), m is the number of grids at the outlet section, and T is the number of days of the lth month. The conversion coefficient used for converting the time unit 'second' to 'day' is 86,400. In the case of backward flow, the flow of the outlet section (Q_{ik}) is negative, and the lake storage capacity ($\sum_{j=1}^{n} \xi_j H_j$) is obtained based on that negative Q_{ik}. Under the condition of numerical simulation, '$Q_{ik} < 0$' and '$Q_{ik} = 0$' have equivalent effects for the WEP. Therefore, when calculating the WEP via Equation (8), if $Q_{ik} < 0$, we set Q_{ik} to 0.

Figure 10 shows a comparison of the monthly WEPs under the S1 and S2 scenarios. According to the figure, the monthly WEPs under the S2 scenario were longer than those under the S1 scenario in the different types of years. The biggest difference in the monthly WEPs was 14.5 d, which appeared in November 2010, followed by 14.4 d and 9.9 d, which appeared in December 2003 and November 2006, respectively. The maximum increase ratio was 47.9% (Table 5), which appeared in September 2006. The next two highest ratios were 43.3% and 43.2%, which appeared in November 2010 and December 2003, respectively. The reason why the maximum increase ratio appeared in September 2006 instead of December 2003 was that the water level of the lake in September 2006 was relatively low and the mean water level of the outlet in September was below 10 m (see Figure 8).

Table 6 lists the differences and the rates of increase in the WEPs under the S1 and S2 scenarios. During the

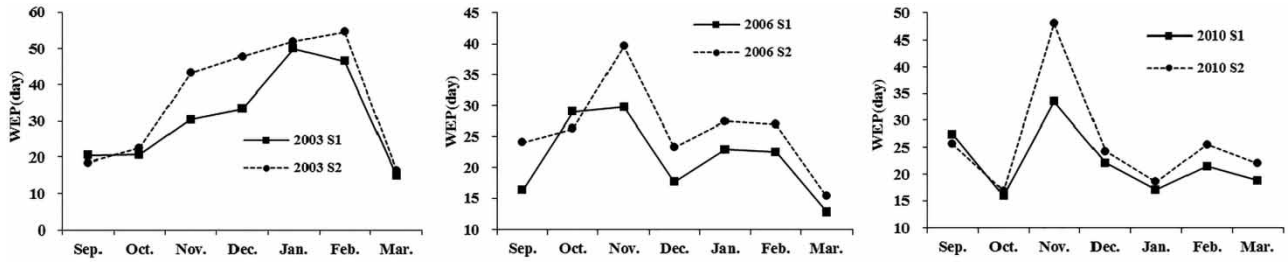

Figure 10 | Monthly WEP in years of different types under the scenarios of S1 and S2.

Table 6 | Comparison of the WEPs in years of different types during water controlling period under S1/S2 (unit: d)

	2003–2004		2006–2007		2010–2011	
Month	**Difference**	**Increase ratio**	**Difference**	**Increase ratio**	**Difference**	**Increase ratio**
Sep.	0.0	0.0	7.8	47.9	0.2	0.7
Oct.	1.9	9.2	0.3	1.0	1.0	6.3
Nov.	12.7	41.6	9.9	33.2	14.5	43.3
Dec.	14.4	43.2	5.6	31.6	2.2	10.0
Jan.	1.9	3.8	4.5	19.7	1.5	8.8
Feb.	8.2	17.6	4.4	19.6	4.1	19.2
Mar.	1.4	9.3	2.5	19.5	3.2	17.0
Nov.–Mar. average	7.7	21.9	5.4	25.6	5.1	22.6
Sep.–Mar. average	5.8	16.7	5.0	23.1	3.8	17.0

water level (10–11 m) controlling period of the PLHP, the water levels under the S1 and S2 scenarios varied greatly. As a consequence, the WEPs varied greatly. Table 5 also lists the mean WEP from November to March of the following year. According to the table, the regulating water level process of the PLHP caused an extension in the mean WEP. The mean WEP was extended by 5.8 d, 5.0 d, and 3.8 d in 2003, 2006, and 2010, respectively. These represent increase rates of 16.7%, 23.1%, and 17.0%, respectively.

Although the number of days in the WEP under the S2 scenario in 2006 (the normal year) was less than that in the dry year (2003) and more than that in the wet year (2010), the extension in 2006 exhibited the maximum rate, which was caused by low water level, small lake storage capacity, and a short WEP in September to October under the S1 scenario. In addition, the lake exhibited a lower water level and increased flow in December of that year (Figure 10). Therefore, the WEP in December was short, and the difference between the WEPs under the S1 and S2 scenarios varied greatly.

CONCLUSION

The construction of the PLHP has caused controversy since its first proposal. Supporters insist that the PLHP will solve economic and environmental problems caused by the long-lasting drought, while opponents have expressed concerns regarding potential harmful effects on bird habitat and water quality. In this paper, a two-dimensional hydrodynamic model was established using the EFDC code to investigate the hydrological effects of the PLHP. Two scenarios (without/with PLHP) were simulated to assess the possible impacts of the proposed PLHP on water level, velocity, lake current, as well as WEP in a typical wet year, normal year, and dry year. Simulation results show that the water level control of 11 m via the PLHP will markedly increase the mean water level of the lake during the low-flow period of Poyang Lake. This will help address the drought problem in the study area. The flow velocity decreased under the scenario of PLHP operation, especially in the waterway towards the Yangtze River to the north of

Tangyin. The PLHP causes minor impacts on the lake region in the vicinity of Changshan Island and in the two natural reserves, due to the relatively high terrain of the lake bed. The construction of the PLHP will weaken the flow field of the lake region near Changshan Island. The PLHP will also lead to occasional disappearance of the backflow field due to the water storage/drainage process. Because of the water level regulation of the PLHP, the flow patterns of the whole lake will be similar in wet, normal, and dry years. The monthly lake WEPs will significantly increase due to the water level regulation of the PLHP, at a maximum of 14.5 d (47.9% in ratio). The decreased water velocity and the extension of the WEP may have certain impacts on lake water quality. However, increases in lake storage capacity are the stated purpose of the water level regulation of the PLHP. Whether the project should proceed depends upon balancing the advantages and disadvantages.

The PLHP has a significant impact on the lake WEP due to increases in water level, increases in storage capacity, and relative reductions of velocity. The monthly lake WEPs during the regulation water level periods in the differing types of years extended by varying degrees. Extension of the WEP may result in certain impacts on lake water quality. However, increase in lake storage capacity is the major cause for the extension of the WEP, and this may also improve the environmental carrying capacity of the lake. Therefore, the degree to which the PLHP-mediated change in lake WEP affects the water quality of the lake requires additional study.

ACKNOWLEDGEMENTS

This work is jointly supported by 973 Program of the National Basic Research Program of China (2012CB417003), the Collaborative Innovation Center for Major Ecological Security Issues of Jiangxi Province and Monitoring Implementation (JXS-EW-00) and the National Natural Science Foundation of China (41561101).

REFERENCES

Feng, L., Hu, C., Chen, X. & Li, R. 2011 Satellite observations make it possible to estimate Poyang Lake's water budget. *Environ. Res. Lett.* **6** (4), 44023.

Feng, L., Hu, C., Chen, X., Cai, X., Tian, L. & Gan, W. 2012 Assessment of inundation changes of Poyang Lake using MODIS observation between 2000 and 2010. *Remote Sens. Environ.* **121**, 80–92.

Ferrari, A., Fraccarollo, L., Dumbser, M., Toro, E. F. & Armanini, A. 2010 Three-dimensional flow evolution after a dam break. *J. Fluid Mech.* **663**, 456–477.

Fu, K., Huang, H., Zhong, R., Wang, X. & Su, B. 2011 Reservoir-induced downstream changes of water, sediment and channel morphology: a literature review. *Acta Geogr. Sinica* **66** (9), 1239–1250 (in Chinese).

Guo, H., Hu, Q., Zhang, Q. & Feng, S. 2012 Effects of the Three Gorges Dam on Yangtze River flow and river interaction with Poyang Lake, China: 2003–2008. *J. Hydrol.* **416**, 19–27.

Hamrick, J. M. 1992 *A Three-Dimensional Environmental Fluid Dynamics Computer Code: Theoretical and Computational Aspects*. The College of William and Mary, Virginia Institute of Marine Science, Special Report 317.

Hu, Q., Feng, S., Guo, H., Chen, G. & Jiang, T. 2007 Interactions of the Yangtze river flow and hydrologic processes of the Poyang Lake, China. *J. Hydrol.* **347**, 90–100.

Hu, C., Shi, W., Hu, L. & Zhou, W. 2012 Simulation study on the impact of Poyang lake hydro-junction projects on nitrogen and phosphorus nutrient in lake region. *Resour. Environ. Yangtze Basin* **21** (6), 749–755 (in Chinese).

Hui, F., Xu, B., Huang, H., Yu, Q. & Gong, P. 2008 Modelling spatial-temporal change of Poyang Lake using multitemporal Landsat imagery. *Int. J. Remote Sens.* **29** (20), 5767–5784.

Krausel, P., Boyle, D. P. & Base, F. 2005 Comparison of different efficiency criteria for hydrological model assessment. *Adv. Geosci.* **5**, 89–97.

Li, J. 2009 Scientists line up against dam that would alter protected wetlands. *Science* **326** (5952), 508–509.

Li, Y., Zhang, Q., Yao, J. & Li, X. 2013 Integrated simulation of hydrological and hydrodynamic processes for lake Poyang catchment system. *J. Lake Sci.* **25** (2), 227–235 (in Chinese).

Li, Y., Zhang, Q., Yao, J., Werner, A. D. & Li, X. 2014 Hydrodynamic and hydrological modeling of the Poyang Lake catchment system in China. *J. Hydrol. Eng.* **19** (3), 607–616.

Liu, Y., Song, P., Peng, J., Fu, Q. & Dou, C. 2011 Recent increased frequency of drought events in Poyang Lake basin, China: climate change or anthropogenic effects? *Hydro-climatol. Variability Change* **344**, 99–104.

Mellor, G. L. & Yamada, T. 1982 Development of a turbulence closure model for geophysical fluid problems. *Rev. Geophys.* **20** (4), 851–875.

Min, Q. 2000 Study on the relationship between shape, water regime and innings of Poyang Lake. *Adv. Water Sci.* **11** (1), 76–81 (in Chinese).

Nikora, V. 2010 Hydrodynamics of aquatic ecosystems: an interface between ecology, biomechanics and environmental fluid mechanics. *River Res. Applications* **26** (4), 367–384.

Obeysekera, J., Kuebler, L., Ahmed, S., Chang, M., Engel, V., Langevin, C., Swain, E. & Wan, Y. 2011 Use of hydrologic and

hydrodynamic modeling for ecosystem restoration. *Crit. Rev. Environ. Sci. Technol.* **41** (S1), 447–488.

Renhua, Y., Jiacong, H., Yan, W., Junfeng, G. & Lingyan, Q. 2015 Modeling the combined impact of future climate and land use changes on streamflow of Xinjiang Basin, China. *Hydrol. Res.* **47** (2), 356–372.

Scott, C. J., Vijayasarathi, J. & David, T. H. 2013 Simulating pH effects in an algal-growth hydrodynamics model. *J. Phycology* **49** (3), 606–615.

Tan, G., Guo, S., Wang, J. & Lv, S. 2013 *Study on the Evolution of Hydrology and Water Resources in Poyang Lake Ecological Economic Zone*. China Water & Power Press, Beijing, China (in Chinese).

Wang, P., Lai, G. & Huang, X. 2014 Simulation of the impact of Lake Poyang project on the dynamic of lake water level. *J. Lake Sci.* **26** (1), 29–36 (in Chinese).

Xin, X., Yin, W. & Ye, M. 2011 Preliminary research on hydrodynamic dispatch method of water blooms in Three Gorges Reservoir region. *Water Resour. Power* **29** (7), 16–18 (in Chinese).

Zhang, Q., Ye, X., Werner, A. D., Li, Y., Yao, J., Li, X. & Xu, C. 2014 An investigation of enhanced recessions in Poyang Lake: comparison of Yangtze River and local catchment impacts. *J. Hydrol.* **517**, 425–434.

Zhou, J., Pan, S. & Falconer, R. A. 2014 Effects of open boundary location on the far-field hydrodynamics of a Severn Barrage. *Ocean Modell.* **73**, 19–29 (in Chinese).

First received 2 September 2015; accepted in revised form 9 May 2016. Available online 14 June 2016